Solid-solid phase equilibria in the binary system cobalt molybdate ($CoMoO_4$)-iron molybdate ($FeMoO_4$) and effect of iron on the phase equilibria

ARTICLE *in* THE JOURNAL OF PHYSICAL CHEMISTRY · NOVEMBER 1992

Impact Factor: 2.78 · DOI: 10.1021/j100202a072

Solid–Solid Phase Equilibria in the Binary System $CoMoO_4$–$FeMoO_4$ and Effect of Fe^{III} on the Phase Equilibria

H. Ponceblanc,[†,‡] J. M. M. Millet,[†] G. Coudurier,[†] O. Legendre,[‡] and J. C. Védrine*,[†]

Institut de Recherches sur la Catalyse, CNRS, 2 Avenue A. Einstein, F-69626 Villeurbanne Cedex, France, and Centre de Recherche d'Aubervilliers, Rhône-Poulenc, 52 Rue de la Haie-Coq, 93308 Aubervilliers Cedex, France *(Received: March 2, 1992; In Final Form: July 16, 1992)*

Solid–solid phase equilibria in the binary system $CoMoO_4$–$FeMoO_4$ have been studied by temperature programmed electrical conductivity measurements (TPEC) and confirmed, in some cases, by differential thermal analysis (DTA), X-ray diffraction, and IR spectroscopy. The results show that two continuous solid solutions exist between the two polymorphic forms of $CoMoO_4$ and $FeMoO_4$ (α and β). Fe^{3+} has been shown to be present in these solid solutions where it substitutes Fe^{2+} and Co^{2+}. At low iron content (up to 20%) this substitution is giving rise to an induction phenomenon. At high iron content the compensation mechanism is presumably the formation of bivalent metal vacancies. The evolution of the temperature of the polymorphic transition with the iron content has been studied. A maximum for this temperature has been observed in the Co rich region (between 12 and 20% of iron) and has been shown to vary with Fe^{3+} content. A phase diagram showing the influence of the Fe^{2+} and Fe^{3+} contents on the phase transition is proposed.

Introduction

Cobalt, nickel, and iron molybdates are frequent constituents of selective oxidation catalysts, particularly for mild oxidation of propene into acrolein.[1-5] Although the studies dealing with these molybdate based catalysts yielded many data, they have been limited by the fact that the number of independent constituents of these solids is high and that the resulting complex phase composition is most of the time not known. Furthermore, these catalysts almost always evolve during the catalytic reaction and their phase composition changes.

For example iron, which is present in the catalysts before catalysis in the form of $Fe_2(MoO_4)_3$, is reduced, at least partially, under the conditions of catalysis, as the ferric molybdate is transformed into $FeMoO_4$ and MoO_3.[6,7]

In order to progress in the analysis and the knowledge of the phase equilibria allowed in these molybdate based catalysts, we have studied the solid–solid phase equilibria in the system $CoMoO_4$–$FeMoO_4$ and the effect of the presence of Fe^{3+} on these equilibria. $CoMoO_4$ and $FeMoO_4$ are, with $NiMoO_4$, the only three bivalent metal molybdates presenting a reversible transition between the two forms α and β usually observed for such compounds.[8] The system $CoMoO_4$–$NiMoO_4$ has previously been studied, and two solid solutions α and β have been shown to be present in the total range of composition with a transition temperature evolving linearly from $CoMoO_4$ to $NiMoO_4$.[9] This study has not been extended to the $CoMoO_4$–$FeMoO_4$, the explosive nature of the phase transformation along with the low enthalpy of the phase transition rendering the system difficult to study.

We have, however, overcome these experimental problems by developing several analytical techniques[10] and by studying the effect of the presence of Fe^{3+}, extending concomitantly the study of the phase equilibria in the quaternary system $CoMoO_4$–$FeMoO_4$–$Fe_2(MoO_4)_3$–Fe_2O_3. The structure of the β form corresponds to the structure of $MnMoO_4$,[8] which is monoclinic (space group $C2/m$) with 6 and 4 as coordination numbers, respectively, for the bivalent cation and the molybdenum. The structure of the α form corresponds to the structure of α-$CoMoO_4$,[11] which is also monoclinic with the same space group. The more compact α structure differs from the β structure in the coordination number of the molybdenum (6 in the α form and 4 in the β form).

Experimental Section

(a) Sample Preparation. The samples have been prepared by precipitation from aqueous solutions. This method led to solids with specific surface area suitable for the evaluation of the catalytic properties. Ammonia was added to an aqueous solution of ammonium heptamolybdate $(NH_4)_6Mo_7O_{24}\cdot 4H_2O$ until pH reached 8.5. The mixture was then boiled for 2 h under argon, until neutral pH was reached. The solution was deoxygenated by bubbling an argon flow for 15 min. A freshly prepared solution of ferrous chloride $FeCl_2\cdot 4H_2O$, with or without cobalt nitrate $Co(NO_3)_2\cdot 6H_2O$, was slowly added to the boiling mixture, which was then boiled for 1 h. The precipitate was filtered, washed by deoxygenated water, and evaporated to dryness under vacuum. The solid obtained was crystalline mixed iron and cobalt ammonium metallomolybdates of the same type as those studied by Pezerat.[12] The precursor was calcined at 450 °C for 10 h under a deoxygenated and dehydrated nitrogen flow. A further calcination at 900 °C for 2 h was performed in order to obtain a better crystallization of the solids. In spite of these repeated precautions, ferric ions were detected in significant amount in the samples. However no ferric phase was detected in the precursors. Consequently, in order to obtain different compositions of ferric iron, samples were reduced by a 5 $dm^3\cdot h^{-1}$ hydrogen flow (1:4) at 400 °C. The α phase was obtained by grinding the β phase obtained by calcination at 450 °C or by heating it at 900 °C and then cooling it rapidly.

Cobalt molybdate, iron molybdate, and mixed cobalt, iron molybdates were noted respectively CM, FM, and CFM.

(b) Chemical Analysis. The cationic composition of the prepared solids was determined by atomic absorption using a 1100 Perkin-Elmer spectrophotometer. Cobalt, iron, and molybdenum contents were respectively detected at 240.7, 248.4, and 313.3 nm. Analysis of ferrous ions was preformed using the following redox reaction: The solids were dissolved in hot concentrated orthophosphoric acid solution under nitrogen flow. After this solution was cooled to room temperature, 0.1 N sulfuric acid was added along with a drop of indicator (barium π-diphenylaminesulfonate). Titration was performed by addition of a 0.02 M potassium bichromate solution.

(c) X-ray Diffraction. An X-ray investigation of the oxide samples was conducted at room temperature, using a D500 Siemens diffractometer. The patterns were obtained using copper radiation at 35 kV and 30 mA with a scanning speed in 2θ of 1° min^{-1}. By computer folding and fitting, the diffraction angles of the patterns have been determined and used to calculate the cell parameters of the corresponding structures. This last operation was performed using a least squares method. Each X-ray diffraction spectrum of CFM samples were treated by a deconvolution program.

(d) Infrared Spectroscopy. The infrared spectra were recorded with a 580 Perkin-Elmer spectrophotometer. The samples were diluted in a KBr matrix (1%) and pressed into wafers.

[†] CNRS. Telefax, 33/72445399; telephone, 33/72445317.
[‡] Centre de Recherche d'Aubervilliers, Rhône-Poulenc.

0022-3654/92/2096-9462$03.00/0

TABLE I: Atomic Compositions of CM, FM, and CFM Samples, Calcined for 10 h at 450 °C, Determined by Chemical Analysis, (CM = $CoMoO_4$, FM = $FeMoO_4$, CFM = $Co_xFe_{1-x}MoO_4$ ($0 < x < 1$); Fe_t = Fe^{2+} + Fe^{3+}

sample	$Co/(Co + Fe_t)$	$Fe_t/(Fe_t + Co)$	$(Co + Fe_t)/Mo$
CM	1	0	0.97
CFM1	0.94	0.06	0.93
CFM2	0.89	0.11	0.93
CFM3	0.88	0.12	0.91
CMF4	0.83	0.17	0.96
CFM5	0.77	0.23	0.98
CFM6	0.75	0.25	0.92
CFM7	0.47	0.53	0.96
CFM8	0.33	0.67	0.97
CFM9	0.14	0.86	0.96
FM	0	1	0.97

TABLE II: Fe^{3+} Concentration as a Function of the Reducing Time of CFM and FM Samples Precalcined at 450 °C, under Hydrogen/Nitrogen Mixture at 400 °C

sample	$Fe_t/(Fe_t + Co)$	reducing time (min)	$Fe^{3+}/(Fe_t + Co)$
CFM1	0.06	0	0.004
CFM2	0.11	0	0.037
		30	0.025
		45	0.014
CFM3	0.12	0	0.026
		60	0.005
CFM4	0.17	0	0.093
		15	0.080
		30	0.021
		60	0.015
CFM5	0.23	0	0.080
		60	0.053
CFM6	0.25	0	0.075
		60	0.039
CFM7	0.53	0	0.254
		60	0.180
CFM8	0.67	0	0.111
		60	#0
CFM9	0.86	0	0.201
		60	0.063
FM	1.00	0	0.16
		180	0.07

(e) Differential Thermal Analysis (DTA). DTA experiments were performed using a MT85 Setaram Analyzer equipped with platinum–rhodium thermocouples. A 20-mg amount of the sample was placed in a 25-μm^3 platinum crucible and analyzed at atmospheric pressure under a deoxygenated and dehydrated nitrogen flow (1 $dm^3 \cdot h^{-1}$). Alumina was used as a reference.

(f) Temperature Programmed Electrical Conductivity Measurements (TPEC). A better determination of the temperature of the polymorphic transitions was achieved by measuring electrical conductivity of a 500-mg sample under an 8-Pa residual air pressure, while temperature was increased at a 5 °C·min^{-1} rate.[10] A constant mechanical pressure of 10^5 Pa was maintained above the sample by a mercury tank. Sample resistance was measured using a Kontron multimeter ($1 < R < 10^6$ Ω) or a Guildine tera-ohmmeter ($10^6 < R < 10^{14}$ Ω).

Results and Discussion

(a) Characterization of the Molybdate Solid Solutions. The compositions of the mixed cobalt and iron molybdates determined by chemical analysis are presented in Table I. A small deviation from ideal stoichiometry ((Co + Fe)/Mo = 1) for the whole set of samples is observed. A thermogravimetric analysis of the CFM3 sample in air during a heating to 900 °C and a subsequent plateau at this temperature showed a small weight loss of 0.3% starting from 700 °C. This weight loss may be due to the sublimation of MoO_3 which could account with analytical errors for the light molybdenum excess detected by chemical analysis. Moreover, chemical analysis shows the presence of ferric iron. As a complement to these observations, the presence of dissolved ferrous and ferric iron has been confirmed by Mössbauer spectroscopy.[14]

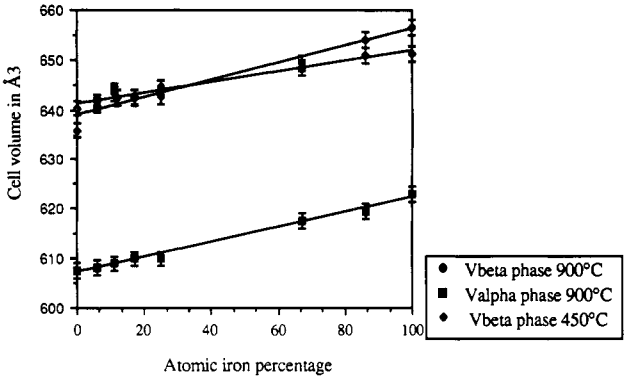

Figure 1. Variation of the cell volumes of α and β phases of CFM samples calcined at 900 °C and of the β phase of CFM calcined at 450 °C, as a function of total iron content.

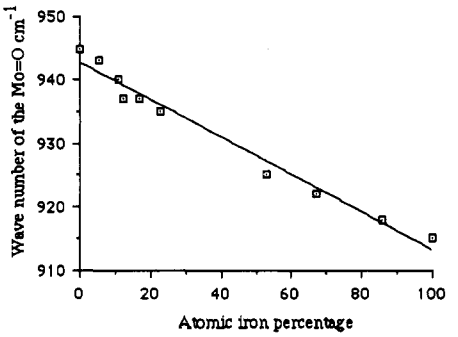

Figure 2. Wavenumber of Mo═O vibration against iron content for α-CM, α-CFM, and α-FM compounds at room temperature.

The amount of Fe^{3+} can be decreased using a heat treatment under hydrogen, as described in the Experimental Section. The results of the reduction experiments as a function of the reducing time (presented in Table II) show that small amounts of ferric iron remain in all cases. Longer heat treatment resulted in the formation of $Fe_2Mo_3O_8$, which contains both reduced iron and molybdenum.

The X-ray diffraction powder patterns of the samples calcined at 900 °C or at 450 °C show the presence of only two phases, α type and β type. When calcined at 900 °C, only α-$CoMoO_4$ was present, whereas CFM and FM showed a mixture of the metastable β phase and the α phase. Unit cell parameters of these two polymorphic forms have been calculated and are reported in Table IIIa,b. For the simple molybdates CM and FM, these values are in good agreement with earlier studies.[15,16] The variation of the cell volumes with the percentage of iron is shown in Figure 1. This variation is in good agreement with Vegard's law, thus suggesting the occurrence of a solid solution of iron into the two polymorphic forms of cobalt molybdate. Although Fe^{3+} was detected unambiguously, it does not seem to be in a quantity large enough to significantly influence the value of these parameters.

IR spectroscopy confirms the results obtained by X-ray diffraction concerning the formation of solid solutions: the wavenumber shift of the Mo═O and the $MoOMe^{2+}$ vibrations with iron content of the mixed molybdates are given in Table IV. These bands are specific for the α-type molybdates since the grinding of the samples for the preparation of the pellets with KBr brings the transformation of the β phase. One can notice in Figure 2 that Mo═O vibration shows a regular shift when iron is substituted for cobalt. This shift corresponds to an increase of the Mo═O bond length, which is in agreement with the increase of the unit cell volume. This observation confirms the existence of a continuous solid solution between $CoMoO_4$ and $FeMoO_4$. On the other hand, no simple correlation has been found between $MoOMe^{2+}$ vibrations and the content of substituting iron.

(b) Evolution of the Temperature of the α/β Phase Transformation. Determination of transition temperatures was very difficult to achieve with accuracy by DTA. This was mainly due to the very weak thermal effects associated with the polymorphic

TABLE III: Calculated Values of the Unit Cell Parameters of CFM, Calcinated in a Controlled Atmosphere, as a Function of Total Iron Content

(a) For α and β Calcinated at 900 °C for 2 h[a]

Fe_t^b/(Fe$_t$ + Co)	a (Å)	b (Å)	c (Å)	β (deg)	V (Å^3)
		α Phase			
0	9.71 (4)	8.84 (5)	7.74 (3)	114.0 (2)	607
[1]0	[1]9.666 (8)	[1]8.854 (8)	[1]7.755 (8)	[1]113.8 (2)	[1]607
0.06	9.71 (7)	8.84 (4)	7.75 (4)	114.0 (3)	608
0.11	9.72 (4)	8.85 (5)	7.75 (3)	114.0 (2)	609
0.17	9.72 (4)	8.86 (5)	7.75 (3)	113.9 (2)	610
0.25	9.72 (4)	8.86 (5)	7.75 (3)	113.9 (2)	610
0.67	9.77 (5)	8.89 (7)	7.77 (4)	113.9 (3)	617
0.86	9.79 (4)	8.91 (4)	7.78 (3)	113.9 (2)	619
1	9.80 (5)	8.93 (5)	7.79 (3)	113.9 (3)	623
[2]1	[2]9.805	[2]8.950	[2]7.660	[2]114.05	[2]614
		β Phase			
0	10.22 (3)	9.26 (3)	7.02 (2)	106.9 (2)	639
[3]0	[3]10.21	[3]9.26	[3]7.02	[3]106.16	[3]639
0.06	10.24 (4)	9.29 (4)	7.04 (3)	106.9 (2)	641
0.11	10.25 (3)	9.31 (4)	7.05 (2)	106.8 (3)	644
0.17	10.24 (3)	9.31 (3)	7.04 (3)	106.8 (3)	643
0.25	10.25 (5)	9.31 (4)	7.04 (3)	106.8 (2)	643
0.67	10.27 (4)	9.34 (3)	7.06 (2)	106.5 (2)	649
0.86	10.28 (4)	9.38 (3)	7.07 (3)	106.3 (2)	654
1	10.29 (3)	9.40 (4)	7.07 (4)	106.2 (3)	656
[2]1	[2]10.290	[2]9.394	[2]7.072	[2]106.31	[2]656

(b) For β Form Calcinated at 450 °C for 10 h

Fe_t^b/(Fe$_t$ + Co)	a (Å)	b (Å)	c (Å)	β (deg)	V (Å^3)
0	10.23 (2)	9.28 (1)	7.04 (1)	106.78 (8)	640
6	10.24 (2)	9.29 (2)	7.04 (1)	106.88 (9)	642
11	10.24 (3)	9.31 (3)	7.04 (1)	106.87 (8)	643
12	10.24 (2)	9.30 (1)	7.05 (1)	106.83 (7)	642
17	10.25 (2)	9.30 (1)	7.04 (1)	106.87 (7)	642
25	10.26 (2)	9.32 (2)	7.05 (1)	106.75 (9)	645
67	10.26 (1)	9.34 (1)	7.06 (1)	106.53 (6)	648
86	10.27 (1)	9.36 (1)	7.06 (1)	106.43 (6)	651
100	10.27 (1)	9.36 (1)	7.06 (1)	106.28 (6)	651

[a] Cell parameters are, as indicated with superscript nos. 1-3, 11, 14, and 15, respectively. [b] $Fe_t = Fe^{2+} + Fe^{3+}$.

TABLE IV: Variation of the Position of the Main Infrared Vibrations of CM, FM, and CFM Compounds Calcined at 900 °C

Fe_t/(Co + Fe_t) (%)	ν(Mo=O) (cm^{-1})	ν(MoOMe^{2+}) (cm^{-1})
0	945	615
5.9	943	680
10.8	940	652
12	937	610
16.6	937	620
23	935	630
53	925	630
67	922	625
86	918	625
100	915	650

transition. The enthalpy changes associated with the phase change for $CoMoO_4$ and $FeMoO_4$ are 3.6 and 0.8 kJ·mol^{-1}, respectively.[17] For samples calcined at 900 °C, the transition temperature was detected efficiently by DTA,[10] whereas for those calcined at 450 °C, DTA signals were always very sluggish, even at high amplification, and the transition temperatures were determined by TPEC measurements. In order to evaluate the influence of dissolved Fe^{3+} on the polymorphic transition temperature of the mixed cobalt and iron molybdates, we have determined this temperature for each sample calcined at 450 °C and reduced to different extents. All these temperatures, as a function of ferrous and ferric iron contents, are reported in Table V. The composition of the studied molybdates can be represented graphically into the section of the quaternary system $CoMoO_4$–$FeMoO_4$–Fe_2O_3–MoO_3, shown in Figure 3 since the overall ratio of molybdenum atoms over bi- and trivalent metallic cations remains constant.

TABLE V: α-Phase to β-Phase Transition Temperatures for CM, FM, and CFM Compounds Calcined at 450 °C, as a Function of Fe^{2+} and Fe^{3+} Contents, Determined by TPEC Measurements

sample	Fe_t/(Co + Fe_t) (%)	Fe^{3+}/(Co + Fe_t) (%)	temp of transition ($\alpha \rightarrow \beta$) (°C)
CM	0	0	405
CFM1	0.06	0.004	380
CFM2	0.11	0.014	418
		0.025	429
		0.037	445
CFM3	0.12	0.005	429
		0.026	435
CFM4	0.17	0.015	406
		0.021	409
		0.080	455
		0.093	474
CFM5	0.23	0.053	438
		0.080	465
CFM6	0.25	0.039	431
		0.075	470
CFM7	0.53	0.180	438
		0.254	436
CFM8	0.67	0.110	399
CFM9	0.86	0.063	391
FM	1.00	0.07	355
		0.16	420

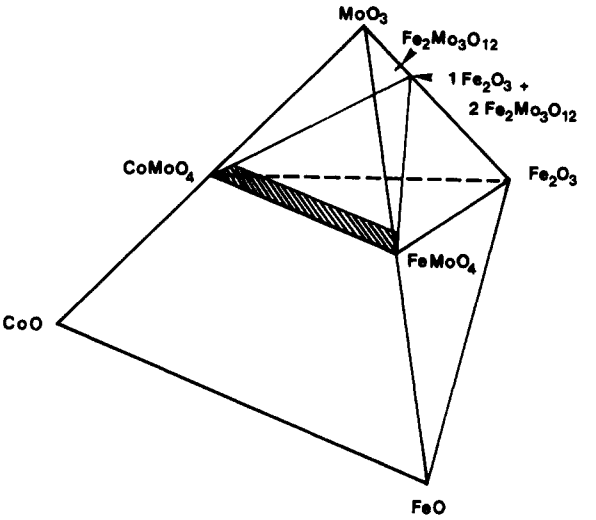

Figure 3. Graphic representation of the compositions of mixed molybdates, into the section of the quaternary system $CoMoO_4$–$FeMoO_4$–Fe_2O_3–MoO_3.

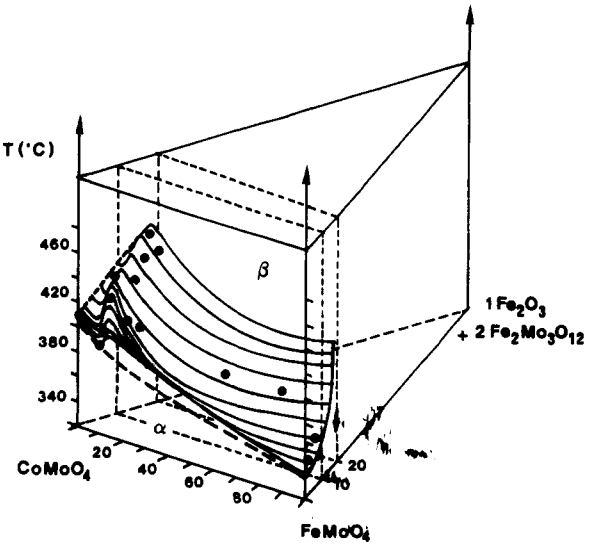

Figure 4. Graphic representation of the phase diagram into the section of the quaternary system $CoMoO_4$–$FeMoO_4$–Fe_2O_3–MoO_3.

The graphic representation of the phase diagram, corresponding to the section of the quaternary system $CoMoO_4$-$FeMoO_4$-Fe_2O_3-MoO_3 characterized by a Mo/bi- and trivalent cations ratio equal to 1 is presented in Figure 4. The ternary phase diagram, thus obtained, shows the existence of a maximal α-phase stability occurring between 12 and 20% iron dissolved into the molybdate. The position of the maximum evolves as a function of the composition toward the limit of the solid solution of Fe^{3+} in pure $CoMoO_4$ which should occur for approximately 20% of Fe^{3+}. It has not been possible to determine this limit since the preparation of such solid solution always led to a solid solution containing Fe^{2+} cations. The limit of the solid solution of Fe^{3+} in the quasi-ternary section corresponds approximately to a Fe^{3+} content equal to 25% since richer samples have been shown to contain ferric oxide and ferric molybdate $Fe_2Mo_3O_{12}$.

The phase transformations of pure ferrous and cobaltous molybdates have not been observed, due to the occurrence of Fe^{3+} in the samples. Thus the phase diagram of the binary system $CoMoO_4$-$FeMoO_4$ was extrapolated from results obtained in the ternary system. This extrapolation corresponds to a nearly linear variation of the phase transition temperatures from $CoMoO_4$ (420 °C) to $FeMoO_4$ (350 °C), as expected.

When Fe^{3+} was dissolved into mixed iron and cobalt molybdates, it always stabilized the α form. This result can be understood since α-phase $CoMoO_4$ is known to crystallize into a more compact lattice than β-phase $CoMoO_4$. So Fe^{3+}, which is a smaller cation compared to Co^{2+} and Fe^{2+}, can substitute and stabilize more easily the most adapted lattice, that is to say the α-$CoMoO_4$ lattice. We have shown in a recent work that the substitution of Fe^{2+} by Fe^{3+} gave rise to an induction valency phenomenon with compounds whose total iron content is less than 20%.[13] At higher iron content the charge compensation of this substitution could be preferentially fixed by the formation of bivalent metal vacancies. It is interesting to note that the limit between the two composition domains corresponds to the position of the maximum for the stabilization of the α phase. Furthermore, it appears that the ferric cations involved in the induction of valency phenomenon are those giving rise to an intervalence charge transfer: $Fe^{3+} \leftrightarrow Fe^{2+} + e^-$. Therefore, substituting iron in cobalt molybdate influences the stabilization of α or β phase in a complex manner leading to the existence of both oxidation states. The presence of one of the two phases α or β, according to the oxidation state of iron, is thought to have a great influence on catalysts performances for mild oxidation reactions.[1]

Conclusion

Substituting ferrous and ferric cations for cobalt into a cobalt molybdate lattice has been achieved by coprecipitation under very mild conditions. It has been shown by X-ray diffraction and infrared spectroscopy that Fe^{2+} enters into cobalt molybdate giving solid solutions for both α and β phases.

Iron also can be present as Fe^{3+} in this solid solution, at least for low contents of iron ($Fe/(Fe + Co) \leq 25\%$). These substitutions were found to have noticeable effect on the temperatures of α-$Co_xFe_{1-x}MoO_4$ to β-$Co_xFe_{1-x}MoO_4$ transitions. All the samples studied contained both ferric and ferrous cations. However the extrapolation from the ternary system which contains the samples to the binary system $CoMoO_4$-$FeMoO_4$ shows that Fe^{2+} stabilized the β phase. On the other hand, Fe^{3+} was found to stabilize the α phase, and a maximal stability of this phase was achieved at a total iron content between 12 and 20% in the ternary system. It was in the same range of composition that a limit of stability of a Fe^{3+} species giving rise to both a charge valence transfer and a phenomenon of induction of valency responsible for a high variation of conductivity was observed.

References and Notes

(1) Wolfs, M. W. J.; Batist, Ph. A. *J. Catal.* **1974**, *32*, 25.
(2) Ueda, W.; Moro-Oka, Y.; Ikawa, T. *J. Catal.* **1981**, *70*, 409.
(3) Matsuura, I. In *Proceedings of the 7th International Congress on Catalysis*; Kodansha—Elsevier: Tokyo—Amsterdam, 1981; Part B, p 1099.
(4) Prasada Rao, T. S. R.; Krishnamurthy, K. R. K. *J. Catal.* **1985**, *95*, 209.
(5) Matsuura, I.; Mizuno, S.; Hashiba, H. *Polyhedron* **1986**, *5*, 111.
(6) Ueda, W.; Moro-Oka, Y.; Ikawa, T.; Matsuura, I. *Chem. Lett.* **1982**, 1365.
(7) Firsova, A. A.; Zurmukhtashvili, M. Sh.; Margolis, L. Ya. *Kinet. Katal.* **1986**, *27*, 1208.
(8) Abrahams, S. C.; Reddy, J. M. *J. Chem. Phys.* **1965**, *43*, 2533.
(9) Get'man, E. I.; Marchenko, V. I. *Zh. Neorg. Khim.* **1980**, *25*, 1933.
(10) Ponceblanc, H.; Millet, J. M. M.; Thomas, G.; Herrmann, J. M.; Védrine, J. C. *J. Phys. Chem.*, following paper in this issue.
(11) Smith, G. W.; Ibers, J. A. *Acta Crystallogr.* **1965**, *19*, 269.
(12) Pezerat, H. *C. R. Acad. Sci. Paris* **1965**, *26*, 5490.
(13) Ponceblanc, H.; Millet, J. M. M.; Coudurier, G.; Herrmann, J. M. Submitted for publication.
(14) Benaichouba, B.; Bussière, P.; Ponceblanc, H. *Hyperfine Interact.* **1990**, *57*, 1741.
(15) Sleight, A. W.; Chamberland, B. L.; Weiher, J. F. *Inorg. Chem.* **1968**, *7*, 1093.
(16) Courtine, P.; Cord, P. P.; Pannetier, G.; Daumas, J. C.; Montarnal, R. *Bull. Soc. Chim. Fr.* **1968**, *12*, 4816.
(17) Courtine, P.; Daumas, J. Ç. *C. R. Acad. Sci. Paris* **1969**, *268*, 1568.